

ORIGINAL ARTICLE

Tracing the Local Volume galaxy halo-to-stellar mass ratio with satellite kinematics

Igor Karachentsev | Olga Kashibadze

Special Astrophysical Observatory,
Russian Academy of Sciences, Russia**Correspondence**I. D. Karachentsev, SAO RAS,
Nizhny Arkhyz, Karachay-Cherkessia,
369167 Russia. Email: ikar@sao.ru**Funding Information**Russian Scientific Foundation, 19–
02–00145.

Rapid advance has been made recently in accurate distance measurements for nearby ($D < 11$ Mpc) galaxies based on the magnitude of the tip of red giant branch stars resolved with the Hubble Space Telescope. We use observational properties of galaxies presented in the last version of Updated Nearby Galaxy Catalog to derive a halo mass of luminous galaxies via orbital motion of their companions. Our sample contains 298 assumed satellites with known radial velocities around 25 Milky Way-like massive galaxies and 65 assumed satellites around 47 fainter dominant galaxies. The average total mass-to- K -band luminosity ratio is $31 \pm 6 M_{\odot}/L_{\odot}$ for the luminous galaxies, increasing up to $\sim 200 M_{\odot}/L_{\odot}$ toward dwarfs. The bulge-dominated luminous galaxies are characterized with $\langle M_T/L_K \rangle = 73 \pm 15 M_{\odot}/L_{\odot}$, while the disc-dominated spirals have $\langle M_T/L_K \rangle = 17.4 \pm 2.8 M_{\odot}/L_{\odot}$. We draw attention to a particular subsample of luminous spiral galaxies with signs of declining rotation curve, which have a radial velocity dispersion of satellites less than 55 km/s and a poor dark matter halo with $\langle M_T/L_K \rangle = 5.5 \pm 1.1 M_{\odot}/L_{\odot}$. We note that a fraction of quenched (dSph, dE) companions around Milky Way-like galaxies decreases with their linear projected separation as $0.75 \exp(-R_p/350 \text{ kpc})$.

KEYWORDS:

(galaxies:) Local Volume – galaxies: halos – galaxies: statistics – galaxies: abundances

1 | INTRODUCTION

According to the standard cosmological model (Λ CDM), most of the mass in galaxies is concentrated in their dark halos which are by one order of magnitude more massive than stellar matter. The ratio of dark mass M_{DM} to stellar mass M_* is different for galaxies with different luminosity. Estimations of M_* are commonly based on K_s luminosity of galaxies, assuming M_*/L_K ratio to be $1.0 M_{\odot}/L_{\odot}$ (Bell et al. 2003) or $0.6 M_{\odot}/L_{\odot}$ (Lelli et al. 2016). According to Kourkchi & Tully (2017), the relation between $\log(M_{\text{DM}}/L_K)$ and $\log(L_K)$ has an asymmetrical V-shaped profile increasing toward reach groups and clusters at $\log(L_K/L_{\odot}) > 10.7$ and toward dwarf galaxies at $\log(L_K/L_{\odot}) < 9.0$. In the intermediate luminosity

zone the characteristic M_{DM}/L_K ratio has the minimal value of $\sim 30 M_{\odot}/L_{\odot}$. Such a behaviour of M_{DM}/M_* vs. M_* is qualitatively consistent with the results of N-body simulations (Sales et al. 2013, Moster et al. 2013, Wechsler & Tinker, 2018). The mass of dark matter in a galaxy cluster is usually determined by virial motions of its members or from the weak lensing effect. Estimations of the full mass of dwarf galaxies are based on the dispersion of radial velocities of stars or few globular clusters (if any).

The relation between M_{DM} and M_* (or L_K) for masses comparable with the stellar mass of the Milky Way is still outlined rather unreliably. The determination of the total mass of a galaxy is most commonly based on data on radial velocities and projected separations of its satellites. Notably, it works for a case of a dynamically isolated galaxy, so the motions of its tiny companions are expected to be Keplerian.

The most suitable objects for determining M_{DM} are nearby bright galaxies surrounded by a retinue of dwarf satellites. In the Local Volume within 11 Mpc there are about 1000 dwarf galaxies most of which have measured radial velocities. Their velocities and projected separations relative to bright galaxies were used to estimate the total masses of galaxies similar to Milky Way (Karachentsev 2005, Karachentsev & Kudrya 2014). Over the last two decades the Hubble Space Telescope performed wholesale measurements of distances to the Local Volume galaxies from luminosities of the tip of red giant branch stars (TRGB) with an accuracy of $\sim 5\%$. It allowed to confidently distinguish between physical satellites of bright galaxies and background or foreground objects. The most full compilation of individual distances of the Local Volume galaxies is presented in the Updated Nearby Galaxy Catalog = UNGC (Karachentsev et al. 2013)¹ and Extragalactic Distance Database = EDD (Anand et al. 2021)². The UNGC catalog contains data on radial velocities, morphological types, K -luminosities and other parameters of galaxies located at distances $D < 11$ Mpc.

In this work we use the most presentable sample of dwarfs swarming around the Local Volume galaxies to determine the total (orbital) mass of galaxies of different luminosity. In Section 2 we present the list of neighboring systems pooled in stacked groups by the luminosity of the central galaxy in different ranges. In Section 3 we consider the relation between the mean ratio M_T/L_K and several parameters of galaxies in groups. In Section 4 a special case of bright galaxies with scanty dark halos is discussed. In Section 5 some properties of early and late type satellites are considered. In the last section we give the concluding remarks. Appendix contains the data on 380 companions of the 23 most bright galaxies of the Local Volume besides the Local Group.

2 | STACKED GROUPS IN THE LOCAL VOLUME

Every galaxy in the UNGC catalog has a dimensionless parameter

$$\Theta_1 = \max(\log(L_i/D_i^3)] + C. \quad i = 1, 2, \dots, N,$$

which is termed the *tidal index*. Here L_i is the luminosity of neighbouring galaxy in the K band and D_i is the distance between the considered galaxy and the neighboring galaxy. Ranging neighbours by the tidal force $F_i \sim L_i/D_i^3$ allows to determine the most significant neighbour, the so-called *main disturber* (MD) which name is also noted in the UNGC for every galaxy. The C constant is adopted in such a way that

a galaxy with $\Theta_1 = 0$ is situated at the *zero velocity sphere* relative to its main disturber. Hence, galaxies with $\Theta_1 < 0$ correspond to the objects of the cosmic expansion field while galaxies with $\Theta_1 > 0$ and the same MD comprise satellite families around their main disturbers. In certain cases of hierarchical structure, the main disturber of a galaxy is coincidentally a companion of a more massive galaxy (for example: SMC as a satellite of LMC, and both Magellanic Clouds are the satellites of the Milky Way). Such a way of clustering galaxies does not impose constraints on radial velocities of supposed group members which could lead to selection effects. The imperfection of this clustering method is the absence of accurate distance estimates for some part of the Local Volume population.

From the resulting sample of groups of different multiplicity (i.e. families around the common main disturber), we have selected for our analysis only the groups with the main galaxy having K luminosity at least twice as high as luminosity of any of its satellites within the virial radius.

To estimate the total (i.e. *orbital*) mass of the main galaxy we used the expression

$$M_{\text{orb}}/M_{\odot} = (16/\pi)G^{-1}\langle\Delta V^2 R_p\rangle = 1.18 \times 10^6 \langle\Delta V^2 R_p\rangle, \quad (1)$$

where G is the gravitational constant, ΔV is the radial velocity difference between the satellite and the central galaxy (km s^{-1}), and R_p is the projected separation of the satellite in kpc (Karachentsev & Kudrya 2014). This relation is based on the assumption that orbits of satellites are oriented randomly and their typical eccentricity is close to $e = 0.7$ according to the numerical simulations (Barber et al. 2014). However, the observational data show that in several nearby groups some part of companions is concentrated into thin planar structures (Ibata et al. 2014, Müller et al. 2018).

Retinues of massive galaxies substantially differ by the number of satellites. According to Karachentsev et al. (2014) the distribution of the parent galaxies by the number of their companions n_{sat} can be approximated by equation

$$N(n_{\text{sat}}) \sim (1 + n_{\text{sat}})^{-2}. \quad (2)$$

Thereby, the abundance of satellites increases from dwarf galaxies to massive ones. According to our data presented in tables below, the mean number of companions with luminosity above $10^7 L_{\odot}$ depends on K luminosity of the main galaxy as

$$n_{\text{sat}} = (L_K/10^{8.8} L_{\odot})^{1/2}. \quad (3)$$

For example, for a galaxy like Milky Way with $L_K = 5 \times 10^{10} L_{\odot}$ the expected number of satellites (brighter than the stated threshold) is $n_{\text{sat}} = 9$, and for dwarf galaxies with $L_K = 1 \times 10^8 L_{\odot}$ there is only one expected companion for

¹<http://www.sao.ru/lv/lvgdb>

²<http://edd.ifa.hawaii.edu>

TABLE 1 Luminous Milky Way-like galaxies in the LV with $\log(L_K/L_\odot) > 10.50$.

Name (1)	T (2)	D (3)	meth (4)	n_v (5)	$\langle R_p \rangle$ (6)	σ_v (7)	$\log L_K$ (8)	$\log M_T$ (9)	M_T/L_K (10)	n_7 (11)	$n_7 e$ (12)	Θ_j (13)	$\log L_1/L_2$ (14)
Milky Way	4	0.01	geom	45	154	109	10.70	12.07	23 ± 8	6	3	1.6	1.28
M 31	3	0.77	cep	51	198	113	10.73	12.23	31 ± 6	15	10	1.4	1.11
NGC 253	5	3.70	trgb	7	465	42	10.98	11.91	9 ± 3	6	2	0.7	1.48
NGC 628	5	10.19	trgb	9	279	69	10.60	12.16	36 ± 13	9	0	-0.5	2.06
NGC 891	3	9.95	trgb	5	325	92	10.98	11.92	9 ± 2	5	0	-0.1	1.01
NGC 1291	1	9.08	trgb	2	254	121	10.97	12.64	47 ± 4	13	10	0.2	1.67
IC 342	6	3.28	cep	8	282	73	10.60	12.20	40 ± 20	7	0	0.5	1.47
NGC 2683	3	9.82	trgb	2	49	43	10.81	11.09	2 ± 2	3	2	-1.2	2.95
NGC 2784	-2	9.82	sbf	5	331	146	10.80	12.96	145 ± 50	20	12	1.0	1.72
NGC 2903	4	9.17	trgb	5	295	41	10.85	11.65	6 ± 5	4	1	-0.8	2.48
M 81	3	3.70	trgb	31	219	123	10.95	12.49	35 ± 10	24	10	1.5	0.36
NGC 3115	-1	9.68	sbf	8	280	112	10.95	12.62	47 ± 19	9	3	0.2	1.68
NGC 3184	6	11.12	SN	2	268	59	10.52	11.82	20 ± 2	3	1	-0.6	2.20
NGC 3521	4	10.70	TF	3	216	55	11.09	11.95	7 ± 3	6	2	-0.2	2.47
NGC 3556	6	9.90	TF	1	202	89:	10.52	12.27:	—	1	0	-0.3	2.85
NGC 4258	4	7.66	trgb	10	268	96	10.92	12.32	25 ± 12	16	7	1.1	1.45
NGC 4594	1	9.55	trgb	15	431	204	11.32	13.19	74 ± 24	23	14	0.2	2.60
NGC 4736	2	4.41	trgb	15	462	68	10.56	12.38	66 ± 22	13	1	0.8	2.37
NGC 5055	4	9.04	trgb	4	216	54	11.00	11.71	5 ± 2	7	1	-0.4	2.54
NGC 5128	-2	3.68	trgb	34	337	124	10.89	12.67	60 ± 18	33	23	1.5	1.14
NGC 5194	5	8.40	SN	5	269	83	10.97	12.13	14 ± 12	8	3	1.3	0.38
NGC 5236	5	4.90	trgb	10	294	61	10.86	12.03	15 ± 4	18	10	0.6	1.98
M 101	6	6.95	trgb	8	281	69	10.79	12.03	17 ± 7	8	2	0.1	1.59
NGC 6744	4	9.51	trgb	5	346	71	10.91	12.19	19 ± 11	9	1	1.1	2.60
NGC 6946	6	7.73	trgb	8	323	65	10.99	12.09	13 ± 5	8	0	0.6	2.59

2–3 galaxies. The empirical relation (3) well agrees with the data obtained by Enger et al (2021) in the TNG50 N-body simulations. Besides that, for early type galaxies (E, S0, Sa) the abundance of observable satellites is greater than about twice the value for late type galaxies. The latter was noted by Javanmardi & Kroupa (2020).

To reduce fluctuation due to the low statistic, we have pooled retinues of galaxies in stacked groups within several ranges by their K luminosity. Table 1 presents the basic parameters of 25 Local Volume groups with main galaxies which luminosities are comparable with the luminosity of the Milky Way and exceeds the threshold of $L_K/L_\odot = 10.50$ dex. Its columns contain: (1) galaxy name; (2) de Vaucouleurs morphological type; (3) galaxy distance in Mpc; (4) method applied to estimate distance: *cep*—from cepheids luminosity, *trgb*—from the tip of the red giant branch, *sbf*—from surface brightness fluctuation, *SN*—from supernovae luminosity, *TF*—from Tully & Fisher relation between the 21 cm line width and the luminosity of a galaxy; (5) number of satellites with radial velocity estimations; (6) mean projected distance of satellites from the main

galaxy in kpc; (7) rms radial velocity of satellites relative to the main galaxy (in km s^{-1}); (8) luminosity of the main galaxy in K band from the UNGC catalog in solar luminosity units; (9) total (orbital) mass estimate for the main galaxy in solar mass units; (10) total mass-to- K luminosity ratio of the galaxy and its statistical error; (11, 12) number of expected satellites with luminosity $L_K/L_\odot > 7.0$ dex and number of early type satellites (dSph, E) among them; (13) logarithmic average K luminosity density within 1 Mpc around the considered galaxy, Θ_j , in global mean density units $4.28 \times 10^8 L_\odot/\text{Mpc}^3$ (Jones et al. 2006); (14) logarithmic ratio between luminosity of the main galaxy and luminosity of its brightest companion situated within the virial zone. As it can be seen from the last column data, nearly all the main galaxies, except M81 and NGC5194, are an order of magnitude or even more brighter than their satellites, corresponding to the model of low-mass test particles moving around the massive central body.

The data on distances, radial velocities and luminosities of 380 supposed companions around the 23 most bright galaxies of the Local Volume besides the Local Group are presented in Appendix Table A1 (available also online³). In addition, we use the properties of 45 Milky Way satellites and 51 M31 satellites from the sample of Kashibadze & Karachentsev (2018) and Putman et al. (2021). The source of extragalactic data is the latest version of the UNGC catalog (<http://www.sao.ru/lv/lvgdb>) supplemented by recent publications (Byun et al. 2020, Karachentsev et al. 2020, Karachentsev & Makarova 2019, Müller & Jerjen 2020, Anand et al. 2021). The UNGC site contains references to original publications introducing the data have been used in this paper.

Galaxies less bright than the Milky Way have only a few satellites. The basic parameters of these galaxies and their companions are listed in Tables 2 – 5. The objects are stacked by K luminosity ranges of main galaxies: [10.0 – 10.5] dex, [9.5 – 10.0] dex, [9.0 – 9.5] dex and < 9.0 dex. The columns of these tables contain: (1) galaxy name fixed in the UNGC catalog; (2) numeric morphological type; (3) distance in Mpc; (4) method applied to estimate distance; satellites without individual distance estimates but supposed to be group members are noted as *mem*; one galaxy has distance estimated from the Numerical Action Method (NAM) model (Shaya et al, 2017); (5) radial velocity of a galaxy relative to the Local Group centroid in km s⁻¹; (6) logarithmic K luminosity in solar luminosity units; (7) projected separation in kpc under the assumption that a satellite has the same distance as the main galaxy; (8) radial velocity of a satellite relative to the main galaxy. The tables include also some supposed companions without having yet measured radial velocities.

As a result, the total number of satellites in our analysis amounts to $N = 564$. Among them 363 companions, or 64%, have measured radial velocities. As it can be seen from presented data, many satellites of neighboring galaxies still miss accurate distance estimates, despite the focused Hubble Space Telescope’s efforts to measure TRGB distances. In that respect the situation beside the Local Volume seems to be even less provided with observational data.

3 | THE TOTAL MASS-TO-LUMINOSITY RATIO AT VARIOUS PARAMETERS OF NEIGHBORING GROUPS.

Mean characteristics of the main galaxies in the neighboring groups are listed in Table 6. Its first column indicates K luminosity range of the dominating galaxy. In the second column we give number of satellites with measured radial velocities used to estimate the orbital (total) mass, M_T . The third column

contains mean radial velocities of satellites relative to the main galaxy. The fourth column specifies mean luminosity of the main galaxy in solar luminosity units. The fifth and the sixth columns are mean projected separation of satellites (kpc) and rms radial velocity of satellites (km s⁻¹) relative to the central galaxy. The last two columns contain mean values of orbital mass (in M_\odot) and orbital mass-to- K luminosity ratio for the main galaxy with mean error estimates.

As it follows from the data listed in the third column, mean radial velocities of satellites agree with the radial velocity of the galaxy, giving the evidence of their physical connection. The agreement of radial velocities within statistical errors is found in every group. The only exception is the NGC2784 group with all 5 satellites having radial velocities exceeding the radial velocity of the main galaxy. These galaxies does not have accurate distance estimates, and the $M_T/L_K = 145M_\odot/L_\odot$ value for this group is extremely large among the groups of Table 1.

According to Tully (2015), the radial velocity dispersion in groups and clusters, σ_v , and the virial mass of these systems, M_T , follow the tight relation

$$\log(M_T/M_\odot) = 6.31 + 3.0 \log(\sigma_v) \quad (4)$$

in the mass range $M_T = (2 \times 10^{12} - 2 \times 10^{15})M_\odot$. Figure 1 reproduces the relation between M_T and σ_v according to our data. The stacked Local Volume groups from Table 6 are depicted by solid circles with error bars. Galaxy groups around the Milky Way and M31 are shown with plus and cross markers, respectively. We have labeled with triangles the nearest Virgo cluster (Kashibadze et al. 2020) and the rich group Leo I at the far periphery of the Local Volume. The Leo I group contains several brightest galaxies of relatively similar luminosity and thus is not included in Table 1. The parameters of the Leo I group are extracted from Karachentsev & Kudrya (2014) and augmented with new data on radial velocities and distances of its members. The relation (4) suggested by Tully (2015) is depicted by dashed line. It agrees quite well with our data and can be remarkably extended to dwarf galaxies area with masses as low as $M_T \sim 3 \times 10^{10}M_\odot$. The radial velocity dispersion of satellites around the Milky Way lays rightward of the relation (4), as we observe predominantly radial motions of satellites from the interior and thereby see their almost full velocity vectors.

Figure 2 reproduces the total mass-to- K luminosity ratio for stacked groups of the Local Volume as a function of luminosities of groups from the Table 6. The curved line on the plot represents Kourkchi & Tully (2017) relation:

$$\log(M_T/L_K) = 1.50 - 0.50 \times \log(L_K/10^{10}L_\odot) \quad \text{at} \quad \log L_K < 9.0 \quad (5)$$

and

$$\log(M_T/L_K) = 1.50 + 0.15 \times \log(L_K/10^{10}L_\odot) \quad \text{at} \quad \log L_K > 10.7$$

³<http://cdsarc.u-strasbg.fr/viz-bin/cat/J/AN/...>

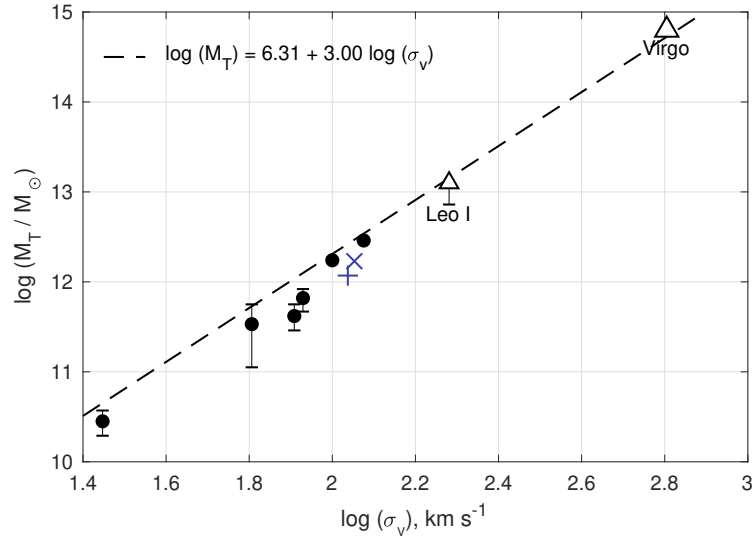


FIGURE 1 Correlation between virial (orbital) mass and radial velocity dispersion. The stacked groups in the Local Volume are presented as solid circles, the Milky Way and M31 galaxies are depicted by plus and cross signs, respectively. The dashed line corresponds to Tully (2015) relation for rich groups and clusters.

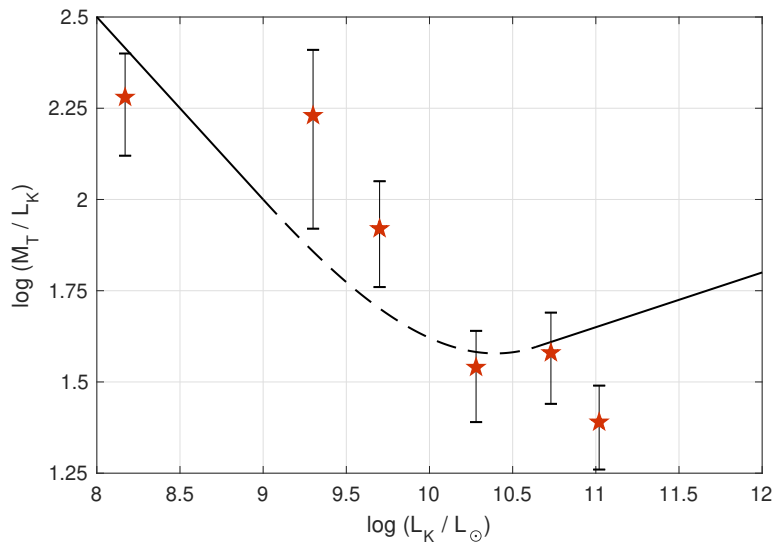


FIGURE 2 Relation between orbital mass and K luminosity for stacked groups in the Local Volume. The curved line reflects the relation obtained by Kourkchi & Tully (2017).

with minimum near $L_K/L_\odot \simeq 10.5$ dex. The stacked groups of the Local Volume generally follow the relation (5), although the minimal value $(M_T/L_K)_{\min} \simeq 25M_\odot/L_\odot$ turns out to be shifted to brighter luminosities, $L_K/L_\odot \simeq 11$ dex. The existence of the minimum suggests that most star formation activity is inherent in galaxies of this specific stellar mass. Note that van Uiteren et al. (2016) have estimated the M_T/M_* ratio for Galaxy And Mass Assembly (GAMA) survey objects augmented with M_T data from Kilo Degree Survey using gravitational lensing effect. They obtained the minimal value

$(M_T/M_*)_{\min} = 41 \pm 10$ with Hubble parameter $H_0 = 73 \text{ km s}^{-1}\text{Mpc}^{-1}$ which is achieved for galaxies with stellar mass $M_*/M_\odot = 10.3$ dex. However, Lapi et al. (2018) and Posti & Fall (2021) relate the minimum value of $M_T/M_* = 20$ to a stellar mass of $M_*/M_\odot = 10.7$ dex.

The literature consistently notes that the amount of dark matter per unit stellar mass is much larger in early type galaxies than in those of late types. Considering the data on radial velocities and projected separations of 214 faint satellites around 2MASS Isolated Galaxies, Karachentseva et al. (2011)

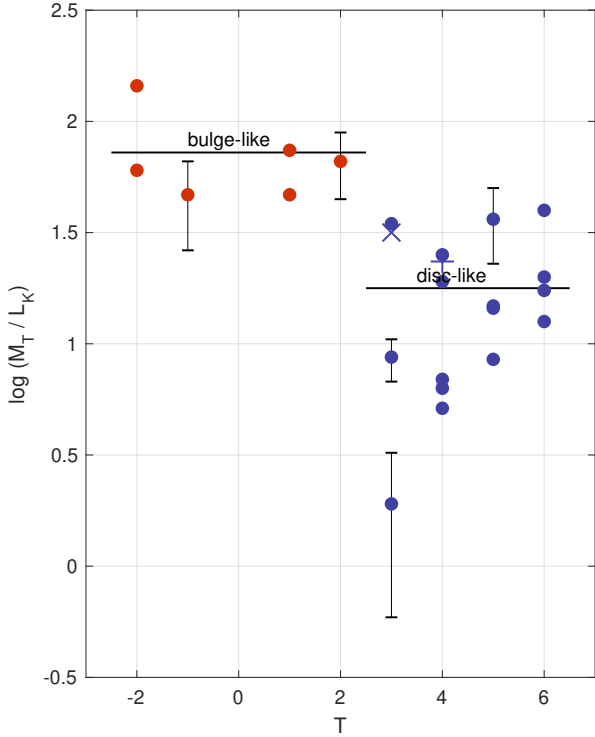


FIGURE 3 Total mass-to- K luminosity ratio for the Local Volume Milky Way-like galaxies of different morphological types. The horizontal lines correspond to the mean values for the bulge-dominated and disc-dominated galaxies. The Milky Way and M31 are depicted by plus and cross signs.

obtained the median value of $M_T/L_K = 64M_\odot/L_\odot$ for E and S0 galaxies, while for spiral galaxies this ratio amounts to $17M_\odot/L_\odot$. The almost four times difference in M_T/L_K is obviously caused by heterogeneous disk and bulge formation histories. According to Correa & Schaye (2020), the difference in M_T/M_* between early and late type galaxies is not so large, amounting only to factor of 1.4. Whereas More et al. (2011), Mandelbaum et al. (2016), Posti & Fall (2021) and Bilicki et al. (2021) get the value (2-4) for this ratio. Moreover, Bilicki et al. (2021) note that for high stellar mass ($M_* > 510^{11}M_\odot$), the red galaxies occupy dark matter halos that are much more massive than those occupied by blue galaxies with the same stellar mass.

The distribution of bright Local Volume galaxies of different types by their M_T/L_K ratio is presented in Figure 3. The vertical bars show standard M_T/L_K errors for several galaxies from Table 1. Early type galaxies with $T < 3$, i.e. E, S0, Sa, have the mean ratio $\langle M_T/L_K \rangle = 73 \pm 15(M_\odot/L_\odot)$, while for galaxies with $T \geq 3$ dominated by disks this ratio makes $17.4 \pm 2.8(M_\odot/L_\odot)$. The difference in M_T/L_K estimates for bulges and disks attains the factor of ~ 4 , significantly exceeding the errors of mean. Our Galaxy (plus sign) and the neighboring

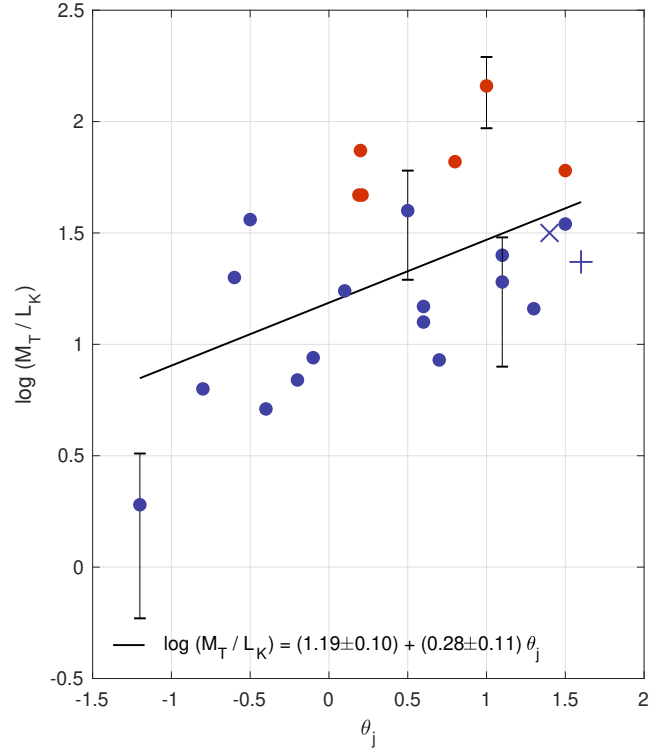


FIGURE 4 Correlation between total mass-to- K luminosity ratio and logarithmic stellar mass density contrast within 1 Mpc around bright galaxies in the Local Volume. Early type galaxies (E, S0, Sa) are marked by red circles. The Milky Way and M31 are shown by plus and cross signs.

galaxy M31 (cross sign) do not seem unique among the disc-like galaxies. Correa & Schaye (2020) suggest that disc-like galaxies, as opposed to bulge-like galaxies with the same halo mass, had more time for gas accretion and formation of more massive stellar subsystem.

The idea that the relation between dark and luminous matter can depend not only on the internal properties of galaxies but also on their environment can be confirmed by data presented in Figure 4. The M_T/L_K relation for galaxies listed in Table 1 is shown as a function of stellar density contrast inside a 1 Mpc sphere centered on the considered galaxy (in the mean cosmic density units). Galaxies of late and early types are depicted as blue and red circles, respectively. It can be seen that early type galaxies are concentrated in the higher density region, $\Theta_j > 0$, having larger M_T/L_K values. In the under-density region, $\Theta_j < 0$, there are only disc-dominated galaxies. Based on the regression line slope, the drop of M_T/L_K ratio from the richest regions to the sparse ones can achieve the factor of ~ 4 . Our galaxy (plus sign) and M31 (cross sign) show an insignificant deviation from the general trend.

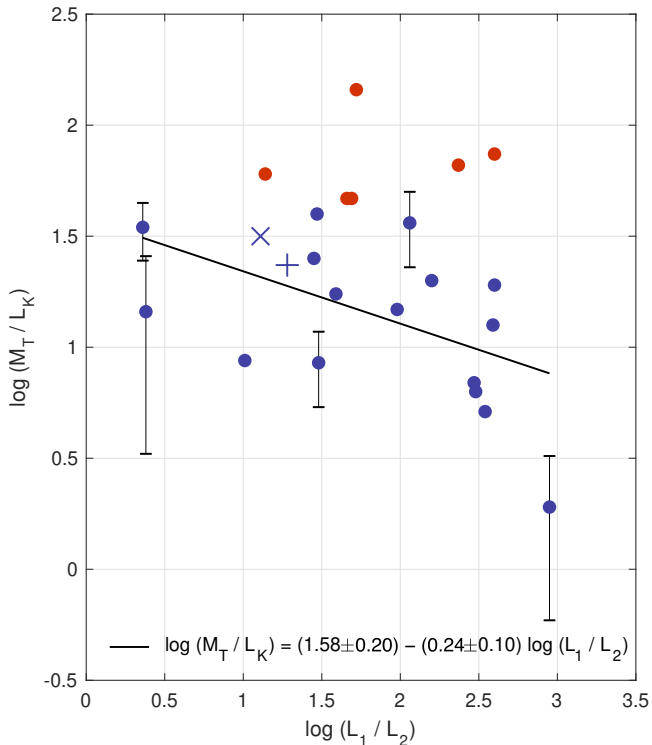


FIGURE 5 Correlation between the total mass-to- K luminosity ratio and the ratio of K luminosities of the main galaxy and its brightest satellite. The designations of galaxies are the same as in Figure 4 .

Wang et al. (2021) examined the abundance of satellites around isolated central galaxies in the Sloan Digital Sky Survey and other surveys. The authors concluded that systems with large difference in luminosities of the central galaxy and its companions have less massive dark halo. Our data on bright isolated Local Volume galaxies are consistent with this prediction. Figure 5 reproduces the relationship between M_T/L_K and the ratio of K luminosities of the main galaxy and its brightest companion located within the virial zone of the main galaxy. The designations are the same as in Figure 4 . The regression line $\log(M_T/L_K) = 1.58 - 0.24 \log(L_1/L_2)$ has a negative slope confirming that the dark halo mass density around the central galaxy tends to decrease while companions become progressively smaller. This effect is mostly expressed for late type spirals (blue circles). The Milky Way and the M31 (plus and cross markers) don't stand out from other bright galaxies of the Local Volume.

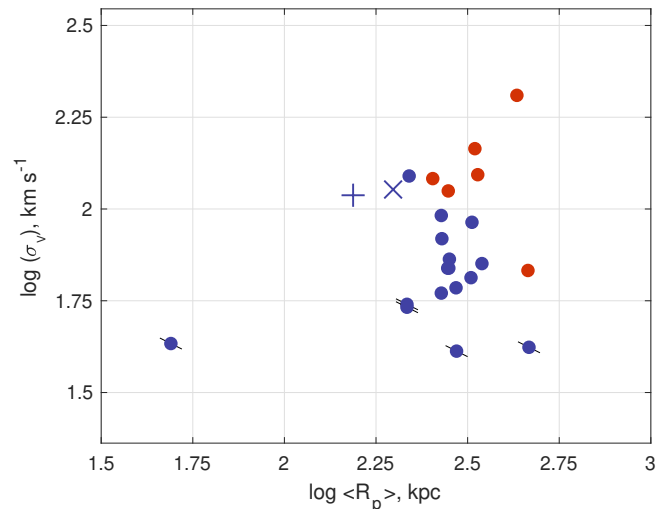


FIGURE 6 Distribution of the Local Volume bright galaxies by the radial velocity dispersion and the mean projected separation of satellites. The designations of galaxies are the same as in previous figure. Galaxies with declining rotation curves are marked by inclined bars.

4 | THE MILKY WAY TYPE GALAXIES WITH POOR DARK HALOS.

The Local Volume galaxies with luminosities $L_K/L_\odot > 10.5$ dex differ significantly from each other by mean satellite system sizes $\langle R_p \rangle$ and their radial velocities dispersions σ_v . The distribution of these Milky Way-like galaxies by $\langle R_p \rangle$ and σ_v is presented in Figure 6 . The designations of early and late type galaxies are the same as in previous figures. This diagram does not show any notable correlation between the system size and velocity dispersion. The galaxies with substantial bulges ($T < 3$, red circles) have nearly the same mean separations of their companions as the disk-dominated galaxies ($T > 2$, blue circles). However, the radial velocity dispersion of bulge-dominated galaxies is on the whole higher than that of disc-dominated galaxies, according to their difference in M_T/L_K value. The evidence for that was provided also by Seo et al. (2020) relying on richer data from SDSS survey. Our Galaxy (plus sign) seems to be untypical on this diagram. But, as we have already noted, σ_v value for the satellites of the Milky Way is slightly higher due to the inner position of the observer and prevailing radial movements of the satellites. On the other hand, the mean distance of the Milky Way satellites turns out to be undervalued because of the abundance of the ultra faint companions seen only at the closest distances. So, the untypical behaviour of our Local group, reported by several authors (Wang et al. 2021), is possibly caused by the selection effects.

According to Casertano & van Gorkom (1991), Lucero et al. (2015) and Zobnina & Zasov (2020), the bright spirals in

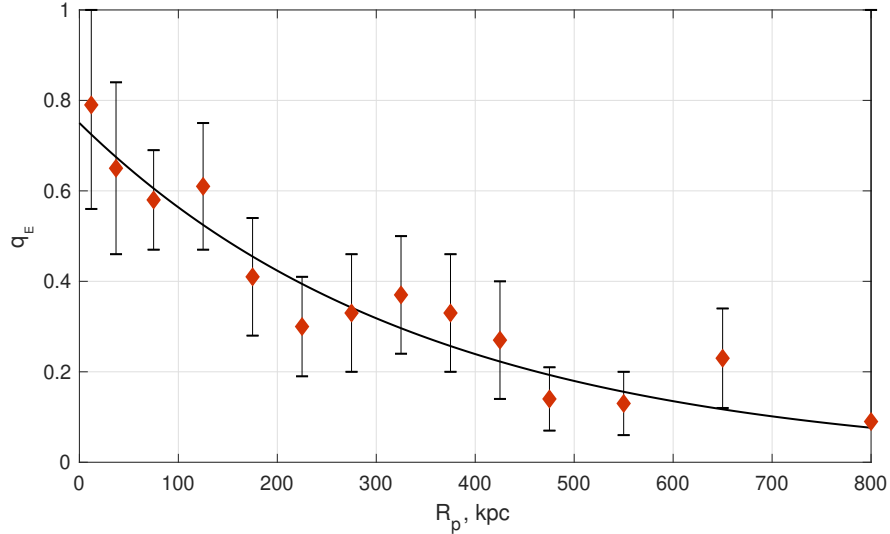


FIGURE 7 Relative number of dwarf satellites brighter than $L_K/L_\odot = 7.0$ dex around the massive Local Volume galaxies as a function of projected separation.

the Local Volume: NGC253, NGC2683, NGC2903, NGC3521 and NGC5055 have declined (quasi-Keplerian) rotation curves at their periphery. These five galaxies are marked in the Figure 6 with strikethrough circles. Karachentsev et al. (2021) give for them mean values: $\log(L_K/L_\odot) = 10.94$, $\sigma_v = 47$ km s $^{-1}$, $\langle R_p \rangle = 248$ kpc, and $\log(M_T/M_\odot) = 11.66$. Their mean total mass-to- K luminosity ratio amounts $\langle M_T/L_K \rangle = 5.8 \pm 1.1$ in solar mass and luminosity units. Such a low value of M_T/L_K points out scanty dark halos around these galaxies corresponding to the decrease of the rotation velocity at the periphery of them. King & Irwin (1997) noted the declined rotation curve for one more spiral galaxy, NGC3556. However, this galaxy has yet only one possible satellite with coarsely measured radial velocity which makes its orbital mass estimate quite indefinite. The existence of massive spiral galaxies with their shallow potential wells raises new unexpected questions with models for the formation and evolution of stellar systems.

Using data on optical and HI rotation curves of spiral galaxies, Lapi et al. (2018), Posti et al. (2019) and Sharma et al. (2021) noted that the halo-mass-to-stellar mass ratio shows a tendency to decrease with increasing stellar mass of the galaxy. This result, obtained on a scale of (1 -2) optical radii of the galaxy, needs to be confirmed by the kinematics of satellites of the host galaxies on the scale of the virial radius of their halos.

5 | EARLY AND LATE TYPE SATELLITES AROUND NEARBY MASSIVE GALAXIES.

While dwarf satellites move through the halo of massive galaxy they lose their gas, which prevents the further star formation in them. This process transforms gas-rich irregular (dIrr) and blue compact dwarfs (BCD) into spheroidal (dSph) and elliptical dwarfs (dE). Obviously, the rate of this transformation increases with closeness of a satellite to the main galaxy, with mass of the main galaxy halo, and with shallowness of the potential well of the satellite itself. Dwarf satellites are better represented in the Local Volume than in more distant volumes, so we have used the existing data to test the expected patterns.

Dozens of ultra faint galaxies with luminosities $L_K \sim (10^2 - 10^5)L_\odot$ were detected within the Local Group (and cannot be observed in more distant groups). To avoid selection effects we have limited ourselves by considering dwarf galaxies with luminosities brighter than $1 \times 10^7 L_\odot$. These objects are thoroughly detectable at the far border of the Local Volume with $D \simeq 10$ Mpc. In the stacked group composed of 25 bright galaxies presented in Table 1 there are 274 satellites more bright than the chosen limit; 118 from them, i.e. 43%, are early type galaxies. The distribution of fraction of the early type satellites along the stacked group radius is shown in Figure 7 by the rhombs with error bars corresponding to the statistical uncertainty. The behaviour of $q_E(R_p)$ is well described by the exponential law

$$q_E(R_p) = 0.75 \times \exp(-R_p/350), \quad (6)$$

where R_p is expressed in kpc. Thus, in the center of the stacked group the relative number of satellites with suppressed star formation amounts to 75%, decreasing twice at the distance $(R_p)_{1/2} = 242$ kpc. The value $(R_p)_{1/2}$ roughly corresponds to the halo virial radius of the massive galaxy with mean luminosity of $L_K = 8 \times 10^{10} L_\odot$. Such a matching is an independent argument for a popular satellite quenching model in which quenched dwarfs are formed while moving through massive neighbouring halo.

The data in Tables 2 –5 show that the relative number of early type satellites falls as the luminosity of the main galaxy decreases. Indeed, the fraction of quenched satellites around the galaxies with luminosities $\log(L_K/L_\odot) = 9.5–10.5$ is 20% (against 43% for Milky Way-like galaxies), while for LMC-like galaxies with $\log(L_K/L_\odot) < 9.5$ this fraction amounts only to $q_E = 10\%$. Hence, the mass of the main halo have a significant impact on the gas abundance and stellar population age of the satellites.

The expected trend of increasing the relative number of dSph and dE dwarfs among less and less massive satellites can be barely tested by observations due to the strong selection bias against faint dwarfs at larger distances. Generally, we can note only that among 174 faint companions with luminosity $\log(L_K/L_\odot) < 7.0$ around bright galaxies from Table 1 the relative number of quenched dwarfs is $q_E = 66\%$, i.e. 1.6 times higher than among brighter companions. The more shallow potential wells of dwarfs facilitate stripping.

In literature there is a large number of works discussing the abundance of satellites around isolated galaxies of different mass and morphology based on N-body simulations within the standard cosmological model (Brook et al. 2014, Sales et al. 2013, Besla et al. 2018, Garrison-Kimmel et al. 2017, Wang et al. 2021, Font et al. 2021). To compare the simulation results and the observational data, the common practice is to use the Local Group or to count the supposed companions around SDSS galaxies. The first case raise the question as to how typical is the Local Group itself. The second case is fraught with the problem of separation of physical satellites from background and foreground galaxies. The sample of 25 massive galaxies of the Local Volume, presented in Table 1, is indicative of diversity characterizing the neighboring groups population.

Figure 8 is a kind of passport for the local groups assembly. The horizontal and the vertical axes correspond respectively to the number of late (n_L) and early (n_E) type satellites around the main galaxies. To avoid the selection of companions by their luminosity due to distance, we consider only satellites brighter than $L_K/L_\odot = 1 \times 10^7$. Main galaxies of late and early types are marked by blue and red circles. Milky Way and M31 are noted by plus and cross signs.

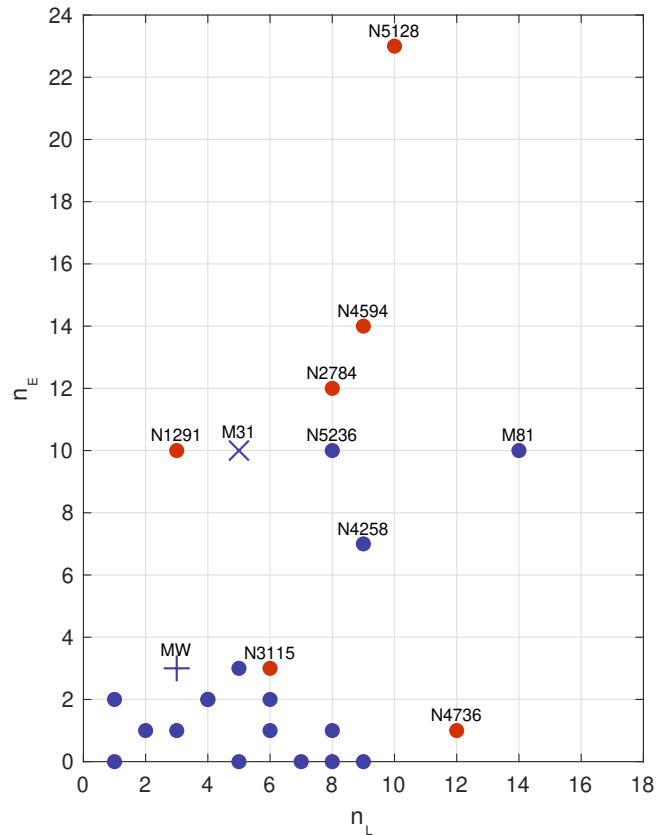


FIGURE 8 Distribution of bright Local Volume galaxies by the number of early and late type satellites brighter than $L_K/L_\odot = 7.0$ dex. The designations of galaxies are the same as in Figure 4 .

As it can be seen from these data, there is a weak positive correlation between numbers of late and early type satellites. The retinues of massive galaxies can be divided conventionally into two classes: poor with $n_E \leq 3$ and rich with $n_E \geq 7$. The first class comprises most retinues around main galaxies of late type including the Milky Way retinue. Main galaxies with dominating bulges are mostly presented in the second class, with M31 ranged among them. This trend is consistent with Wang et al. (2021) stating that retinues of blue SDSS galaxies more likely contain blue satellites because their dark halos are less massive than the halos of red galaxies.

The data of Figure 8 can not imply that the satellite systems around the Milky Way and M31 are atypical for the Local Volume galaxies.

It should be noted that the configuration of galaxies in the Figure 8 may be revised when the outskirts of the neighboring massive galaxies are studied consistently up to specified values of luminosity and surface brightness of satellites, and within specified projected separation of about $\sim (1 - 2)$ virial

radii of the main galaxy halo. The progress in measuring accurate distances of satellites also can make some difference to the pattern of this plot.

6 | CONCLUDING REMARKS.

We used the data from the UNGC catalog (Karachentsev et al. 2013) to select satellites around relatively isolated galaxies in the Local Volume. The sample contains 476 supposed companions around 25 Milky Way-like galaxies with luminosities of $L_K/L_\odot \geq 10.5$ dex and 88 supposed companions around 47 main galaxies of smaller luminosities. About 64% of these satellites have measured radial velocities. Based on projected separations and radial velocities of satellites, we determined the orbital masses (i.e. halo masses) of the central galaxies. For the Milky Way-like galaxies the mean total mass-to- K luminosity ratio is $\langle M_T/L_K \rangle = 31.3 \pm 6.3$ in the solar mass and luminosity units. The mean M_T/L_K ratio shows the systematic grow towards low luminosity galaxies. Early type galaxies (E, S0, Sa) have the total mass per K luminosity unit four times higher than late type spirals (Sb, Sc, Sd), being respectively $\langle M_T/L_K \rangle = 73 \pm 15 (M_\odot/L_\odot)$ and $17.4 \pm 2.8 (M_\odot/L_\odot)$. The M_T/L_K ratio increases as the mean stellar density produced by the neighboring galaxies within a sphere of 1 Mpc grows. Also, the low M_T/L_K ratio is more characteristic of the galaxies having luminosities one or two orders higher than luminosities of their satellites. The minimal radial velocity dispersion values $\sigma_v < 55 \text{ km s}^{-1}$ are found for 5 spirals of the Local Volume: NGC253, NGC2683, NGC2903, NGC3521 and NGC5055, all demonstrating declining rotation curves. Their mean M_T/L_K ratio is surprisingly small, $(5.8 \pm 1.1) M_\odot/L_\odot$, and is comparable with the cosmic dark-to-baryonic matter ratio, $M_{\text{DM}}/M_* \approx 6$.

The fraction of early type satellites (dSph, dE) falls as the luminosity of the central galaxy decreases and grows as the luminosities of the satellites themselves decrease. For the stacked retinue of companions around the Milky Way-like galaxies the relative number of quenched satellites amounts to $\sim 75\%$ in the center, falling exponentially with the distance from the parent galaxy with the decay constant of $\langle R_p \rangle = 350 \text{ kpc}$. These characteristics of the quenched satellite subsystem are quite consistent with the stripping model in which satellites lose their gas while moving through the massive central halo.

Considering the satellites with luminosities $L_K/L_\odot > 7.0$ dex around 25 bright isolated galaxies in the Local Volume with $L_K/L_\odot \geq 10.5$ dex, we conclude that our Galaxy and M31 galaxy seem to be quite typical in abundance of satellites, in their morphology and kinematics.

Acknowledgements. This work is supported by the **Russian Scientific Foundation** grant No. 19–02–00145.

REFERENCES

- Anand, G. S., Rizzi, L., Tully, R. B. et al. 2021, August, *AJ*, 162(2), 80. doi:
- Barber, C., Starkeburg, E., Navarro, J. F., McConnachie, A. W., & Fattahi, A. 2014, January, *MNRAS*, 437(1), 959-967. doi:
- Bell, E. F., McIntosh, D. H., Katz, N., & Weinberg, M. D. 2003, December, *ApJS*, 149(2), 289-312. doi:
- Besla, G., Patton, D. R., Stierwalt, S. et al. 2018, November, *MNRAS*, 480(3), 3376-3396. doi:
- Bilicki, M., Dvornik, A., Hoekstra, H. et al. 2021, January, *arXiv e-prints*, arXiv:2101.06010.
- Brook, C. B., Di Cintio, A., Knebe, A., Gottlöber, S., Hoffman, Y., Yepes, G., & Garrison-Kimmel, S. 2014, March, *ApJ*, 784(1), L14. doi:
- Byun, W., Sheen, Y.-K., Park, H. S. et al. 2020, March, *ApJ*, 891(1), 18. doi:
- Casertano, S., & van Gorkom, J. H. 1991, April, *AJ*, 101, 1231. doi:
- Correa, C. A., & Schaye, J. 2020, December, *MNRAS*, 499(3), 3578-3593. doi:
- Engler, C., Pillepich, A., Pasquali, A. et al. 2021, January, *arXiv e-prints*, arXiv:2101.12215.
- Font, A. S., McCarthy, I. G., & Belokurov, V. 2021, July, *MNRAS*, 505(1), 783-801. doi:
- Garrison-Kimmel, S., Wetzel, A., Bullock, J. S. et al. 2017, October, *MNRAS*, 471(2), 1709-1727. doi:
- Ibata, R. A., Ibata, N. G., Lewis, G. F. et al. 2014, March, *ApJ*, 784(1), L6. doi:
- Javanmardi, B., & Kroupa, P. 2020, March, *MNRAS*, 493(1), L44-L48. doi:
- Jones, D. H., Peterson, B. A., Colless, M., & Saunders, W. 2006, June, *MNRAS*, 369(1), 25-42. doi:
- Karachentsev, I. D. 2005, January, *AJ*, 129(1), 178-188. doi:
- Karachentsev, I. D., Kaisina, E. I., & Makarov, D. I. 2014, January, *AJ*, 147(1), 13. doi:
- Karachentsev, I. D., & Kudrya, Y. N. 2014, September, *AJ*, 148(3), 50. doi:
- Karachentsev, I. D., Makarov, D. I., & Kaisina, E. I. 2013, April, *AJ*, 145(4), 101. doi:
- Karachentsev, I. D., & Makarova, L. N. 2019, September, *Astrophysics*, 62(3), 293-299. doi:
- Karachentsev, I. D., Makarova, L. N., Brent Tully, R., Anand, G. S., Rizzi, L., & Shaya, E. J. 2020, November, *A&A*, 643, A124. doi:
- Karachentsev, I. D., Tully, R. B., Anand, G. S., Rizzi, L., & Shaya, E. J. 2021, April, *AJ*, 161(4), 205. doi:
- Karachentseva, V. E., Karachentsev, I. D., & Melnyk, O. V. 2011, October, *Astrophysical Bulletin*, 66(4), 389-406. doi:
- Kashibadze, O. G., & Karachentsev, I. D. 2018, January, *A&A*, 609, A11. doi:
- Kashibadze, O. G., Karachentsev, I. D., & Karachentseva, V. E. 2020, March, *A&A*, 635, A135. doi:
- King, D., & Irwin, J. A. 1997, August, *New A*, 2(3), 251-276. doi:
- Kourkchi, E., & Tully, R. B. 2017, July, *ApJ*, 843(1), 16. doi:
- Lapi, A., Salucci, P., & Danese, L. 2018, May, *ApJ*, 859(1), 2. doi:
- Lelli, F., McGaugh, S. S., & Schombert, J. M. 2016, December, *AJ*, 152(6), 157. doi:
- Lucero, D. M., Carignan, C., Elson, E. C., Randriamampandry, T. H., Jarrett, T. H., Oosterloo, T. A., & Heald, G. H. 2015, July, *MNRAS*, 450(4), 3935-3951. doi:

- Mandelbaum, R., Wang, W., Zu, Y., White, S., Henriques, B., & More, S. 2016, April, *MNRAS*, 457(3), 3200-3218. doi:
- More, S., van den Bosch, F. C., Cacciato, M., Skibba, R., Mo, H. J., & Yang, X. 2011, January, *MNRAS*, 410(1), 210-226. doi:
- Moster, B. P., Naab, T., & White, S. D. M. 2013, February, *MNRAS*, 428(4), 3121-3138. doi:
- Müller, O., & Jerjen, H. 2020, December, *A&A*, 644, A91. doi:
- Müller, O., Pawlowski, M. S., Jerjen, H., & Lelli, F. 2018, February, *Science*, 359(6375), 534-537. doi:
- Posti, L., & Fall, S. M. 2021, May, *A&A*, 649, A119. doi:
- Posti, L., Fraternali, F., & Marasco, A. 2019, June, *A&A*, 626, A56. doi:
- Putman, M. E., Zheng, Y., Price-Whelan, A. M., Grcevich, J., Johnson, A. C., Tollerud, E., & Peek, J. E. G. 2021, May, *ApJ*, 913(1), 53. doi:
- Sales, L. V., Wang, W., White, S. D. M., & Navarro, J. F. 2013, January, *MNRAS*, 428(1), 573-578. doi:
- Seo, G., Sohn, J., & Lee, M. G. 2020, November, *ApJ*, 903(2), 130. doi:
- Sharma, G., Salucci, P., & van de Ven, G. 2021, May, *arXiv e-prints*, arXiv:2105.13684.
- Shaya, E. J., Tully, R. B., Hoffman, Y., & Pomarède, D. 2017, December, *ApJ*, 850(2), 207. doi:
- Tully, R. B. 2015, February, *AJ*, 149(2), 54. doi:
- van Uitert, E., Cacciato, M., Hoekstra, H. et al. 2016, July, *MNRAS*, 459(3), 3251-3270. doi:
- Wang, W., Takada, M., Li, X. et al. 2021, January, *MNRAS*, 500(3), 3776-3801. doi:
- Wechsler, R. H., & Tinker, J. L. 2018, September, *ARA&A*, 56, 435-487. doi:
- Zobnina, D. I., & Zasov, A. V. 2020, April, *Astronomy Reports*, 64(4), 295-309. doi:

TABLE 2 Sub-MW-like galaxies in the LV with $\log(L_K/L_\odot) = 10.0 - 10.5$ and their companions.

Name	T	D	meth	V_{LG}	$\log L_K$	R_p	ΔV
NGC 925	7	9.55	trgb	738	10.14	0	0
d0226+3325	10	9.55	mem	705	7.34	28	-33
AGC 124640	10	9.55	mem	834	7.14	63	96
DDO 25	8	9.55	mem	785	8.89	210	47
DDO 19	10	9.55	mem	771	8.03	422	33
UGCA 127	6	8.50	TF	562	10.00	0	0
UGCA 127 sat	10	8.50	mem	538	8.76	24	-24
HIPASSJ0622-07	8	8.40	TF	591	9.45	108	29
NGC 2787	1	7.48	sbf	842	10.19	0	0
UGC 4998	9	8.24	trgb	770	8.71	128	-72
NGC 3344	4	9.82	trgb	500	10.33	0	0
NGC 3344 dw1	10	9.82	mem	—	6.29	34	—
NGC 4490	7	8.91	mem	623	10.28	0	0
NGC 4485	8	8.91	trgb	517	8.99	9	-106
MAPS1231+42	10	8.91	mem	602	7.06	72	-21
[KK98] 149	10	8.51	trgb	445	8.15	98	-178
DDO 129	8	8.90	TF	582	8.81	197	-41
NGC 4517	7	8.36	trgb	978	10.27	0	0
dw 1232+0015	-1	8.36	mem	1036	7.67	22	58
CGCG 014-054	9	9.60	TF	954	8.01	238	-24
NGC 4559	6	8.91	trgb	787	10.20	0	0
AGC 220847	9	9.18	TF	777	7.72	264	-10
NGC 4631	7	7.35	trgb	581	10.49	0	0
NGC 4627	-3	7.30	mem	541	9.50	5	-40
NGC 4631 dw2	10	7.30	mem	—	6.62	10	—
NGC 4631 dw3	-2	7.30	mem	—	6.84	23	—
BTS 151	-2	7.35	sbf	734	7.75	36	153
PGC 100707	10	7.30	mem	693	7.45	41	112
NGC 4631 dw1	10	7.30	mem	—	7.30	46	—
HSC-9	-1	7.05	sbf	—	7.07	47	—
KDG 178	10	7.30	mem	763	7.16	55	162
HSC-10	-1	7.05	sbf	—	6.83	74	—
[KK98] 141	10	7.11	trgb	568	6.98	542	-13
NGC 4826	2	4.41	trgb	365	10.49	0	0
[KK98] 177	-2	4.83	trgb	228	7.42	132	-137
UGC 7929	9	4.40	mem	334	7.01	205	-31
[KK98] 180	-2	4.40	mem	—	7.36	335	—
DDO 154	10	4.04	trgb	354	7.59	426	-11
IC 5201	6	8.80	TF	893	10.01	0	0
AM 2220-460	10	8.80	mem	822	7.62	78	-71



TABLE 3 M33-like galaxies in the LV with $\log(L_K/L_\odot) = 9.5 - 10.0$ and their companions.

Name	T	D	meth	V_{LG}	$\log L_K$	R_p	ΔV
M 33	6	0.93	trgb	34	9.62	0	0
And XXII	-3	0.79	trgb	87	5.28	47	53
NGC 1313	7	4.31	trgb	264	9.57	0	0
[KK98] 27	10	4.23	trgb	327	7.04	25	63
NGC 2283	6	10.0	TF	622	9.84	0	0
KKSG 9	9	10.0	mem	474	8.72	63	-148
IC 2171	8	9.90	TF	572	9.05	77	-50
NGC 2403	6	3.19	trgb	262	9.86	0	0
MADCASHJ0742+65	-2	3.39	trgb	—	5.86	36	—
DDO 44	-3	3.21	trgb	356	7.78	73	94
NGC 2366	9	3.28	trgb	251	8.70	206	-11
ESO 495-021	9	8.24	trgb	581	9.56	0	0
ESO 496-010	9	8.59	trgb	524	8.43	415	-57
CGMW2-3473	9	7.40	TF	549	8.31	431	-32
NGC 3432	8	9.20	TF	587	9.64	0	0
LV J1052+3628	10	9.20	mem	451	7.04	8	-136
UGC 5983	10	9.20	mem	741	7.80	10	154
LV J1052+3639	10	9.20	mem	487	7.88	27	-100
VV 747	10	9.20	mem	594	8.02	180	7
NGC 4236	8	4.41	trgb	157	9.61	0	0
[KK98] 125	10	4.40	mem	—	6.61	50	—
DDO 165	9	4.83	trgb	196	8.23	374	39
NGC 4449	8	4.27	trgb	249	9.68	0	0
LV J1228+4358	-1	4.07	trgb	273	8.53	11	24
NGC 4656	8	7.98	trgb	635	9.93	0	0
NGC 4656UV	10	7.98	mem	568	8.88	40	-67
NGC 5068	6	5.15	trgb	469	9.73	0	0
dw 1318-21	-1	4.90	mem	—	7.06	78	—
NGC 6503	6	6.25	trgb	309	10.00	0	0
[KK98] 242	10	6.47	trgb	—	6.44	31	—
NGC 7640	5	8.43	trgb	668	9.77	0	0
UGC 12588	8	8.43	mem	723	8.83	103	55
DDO 217	8	8.55	TF	720	9.37	219	52
NGC 7793	6	3.63	trgb	250	9.70	0	0
PGC 704814	10	3.60	mem	299	6.90	14	49

TABLE 4 LMC-like galaxies in the LV with $\log(L_K/L_\odot) = 9.0 - 9.5$ and their companions.

Name	T	D	meth	V_{LG}	$\log L_K$	R_p	ΔV
NGC 24	5	7.31	trgb	606	9.48	0	0
dw 0009-25	-1	7.31	mem	—	6.00	14	—
dw 0010-25	-1	7.31	mem	—	7.39	52	—
NGC 404	-1	2.98	trgb	193	9.26	0	0
Do-I	-2	3.31	trgb	—	6.48	62	—
NGC 1156	8	6.98	trgb	507	9.21	0	0
NGC 1156 dw1	10	6.98	mem	—	6.55	17	—
NGC 1156 dw2	10	6.98	mem	—	6.41	22	—
LV J0300+2546	10	6.98	mem	443	7.24	71	-64
dw 0301+2446	10	6.98	mem	—	6.57	74	—
AGC 124056	10	6.98	mem	538	6.57	186	31
NGC 1569	8	3.19	trgb	106	9.40	0	0
UGCA 92	10	3.22	trgb	93	8.04	69	-13
NGC 1744	7	10.00	TF	574	9.42	0	0
ESO 486-021	9	10.00	mem	664	8.74	167	90
LMC	9	0.05	cep	28	9.42	0	0
SMC	9	0.06	cep	-22	8.85	18	-50
NGC 2337	9	11.86	trgb	476	9.34	0	0
UGC 3698	10	11.27	trgb	464	8.36	37	-12
NGC 2337 dw TBG1	9	11.9	mem	—	7.14	72	—
NGC 4214	8	2.88	trgb	295	9.00	0	0
KDG 90	-2	2.98	trgb	—	7.59	9	—
NGC 4190	9	2.83	trgb	239	7.90	25	-56
NGC 4163	9	2.99	trgb	163	7.92	36	-132
MADCASH-2	10	3.00	trgb	—	5.80	70	—
NGC 5474	8	6.98	trgb	424	9.21	0	0
PGC 2448110	10	6.98	mem	392	7.02	4	-32

TABLE 5 Dwarf galaxies with $\log(L_K/L_\odot) < 9.0$ in the LV and their companions.

Name	T	D meth	V_{LG}	$\log L_K$	R_p	ΔV
NGC 185	-3	0.66 trgb	73	8.36	0	0
NGC 147	-3	0.76 trgb	85	8.21	11	12
UGC 2716	8	6.66 trgb	467	8.36	0	0
UGC 2684	10	7.08 trgb	438	7.57	112	-29
ESO 121-020	10	6.08 trgb	319	7.78	0	0
LV J0616-5745	10	6.1 mem	286	7.07	6	-33
DDO 47	8	8.17 trgb	160	8.74	0	0
[KK98] 65	10	7.98 trgb	170	8.11	40	10
CGCG 262-028	9	9.80 TF	497	8.18	0	0
KKH 40	10	9.25 trgb	510	7.65	25	13
UGC 5186	10	9.40 TF	496	7.71	0	0
AGC 198691	10	10.91 NAM	464	6.42	37	-32
DDO 64	10	10.91 TF	461	8.41	0	0
[KK98] 78	10	10.9 mem	479	7.29	6	18
NGC 3109	8	1.34 trgb	110	8.58	0	0
Antlia	10	1.37 trgb	66	6.50	29	-44
Antlia B	10	1.29 trgb	82	6.09	78	-28
[KK98] 94	10	10.19 trgb	684	7.32	0	0
LeG 21	10	10.4 mem	696	6.90	7	12
LV J1157+5638	10	8.75 trgb	514	7.33	0	0
LV J1157+5638 sat	10	8.75 mem	—	5.84	5	—
UGC 7584	9	6.14 mem	545	7.40	0	0
KKH 80	10	6.14 trgb	542	7.14	21	-3
dw 1243-42	-1	3.60 mem	—	6.68	0	0
dw 1243-42b	10	3.60 mem	—	6.26	1	—
NGC 4688	6	6.70 TF	855	8.50	0	0
[KK98] 164	8	6.71 TF	910	7.85	13	55
dw 1252-40	-1	3.60 mem	—	7.37	0	0
dw 1251-40	-1	3.60 mem	—	6.26	4	—
DDO 161	8	6.03 trgb	545	8.74	0	0
UGCA 319	10	5.75 trgb	555	8.02	32	10
DDO 168	10	4.25 trgb	270	8.13	0	0
DDO 167	10	4.25 trgb	230	7.19	34	-40
DDO 169	10	4.41 trgb	348	7.73	0	0
DDO 169 NW	10	4.33 trgb	328	6.34	4	-20

TABLE 6 Mean parameters of the primary galaxies and their suites in the LV.

L_K of primary	N_{sat}	$\langle \Delta V \rangle$	$\log \langle L_K \rangle$	$\langle R_p \rangle$	$\langle \sigma_V \rangle$	$\log \langle M_T \rangle$	$\log \langle M_T / L_K \rangle$
(10.9–11.4) dex	106	$+25 \pm 14$	11.02	307	119	12.46	$1.39^{+.10}_{-.13}$
(10.5–10.9) dex	192	$+4 \pm 9$	10.73	260	100	12.24	$1.58^{+.11}_{-.14}$
(10.0–10.5) dex	23	-7 ± 20	10.28	151	85	11.82	$1.54^{+.10}_{-.15}$
(9.5–10.0) dex	16	-7 ± 19	9.70	125	81	11.62	$1.92^{+.13}_{-.16}$
(9.0–9.5) dex	9	-26 ± 23	9.30	68	64	11.53	$2.23^{+.18}_{-.31}$
(7.0–9.0) dex	15	-6 ± 7	8.17	30	28	10.45	$2.28^{+.12}_{-.16}$



APPENDIX A: DATA

TABLE A1 The data on distances, radial velocities and luminosities of 380 supposed companions around the 23 most bright galaxies of the Local Volume besides the Local Group.

Name	T	D	meth	V_{LG}	$\log L_K$	R_p	ΔV
NGC 253	5	3.70	trgb	276	10.98	0	0
Scl-MM-Dw2	-2	3.12	trgb	—	7.36	53	—
Scl-MM-Dw1	-2	3.94	trgb	—	6.77	72	—
LV J0055-2310	10	3.62	trgb	288	6.17	176	12
Sculptor SR	10	3.70	mem	—	6.36	258	—
DDO 6	10	3.43	trgb	347	7.08	278	71
NGC 247	7	3.71	trgb	210	9.50	293	-66
Sc 22	-3	4.29	trgb	—	7.15	349	—
ESO 540-032	10	3.63	trgb	285	6.83	351	9
KDG 2	10	3.56	trgb	290	6.85	468	14
ESO 349-031	10	3.21	trgb	234	7.12	814	-42
NGC 7793	6	3.71	trgb	250	9.70	846	-26
NGC 628 = M74	5	10.19	trgb	827	10.60	0	0
NGC 628 dwB	10	10.2	mem	—	5.30	34	—
NGC 628 dwA	10	10.2	mem	—	7.03	37	—
UGC 1171	10	10.2	mem	906	8.09	132	79
DDO 13	10	9.04	bs	798	8.53	149	-29
AGC 112503	9	10.2	mem	909	7.15	155	82
NGC 628 dw TBG	10	10.2	mem	—	6.78	174	—
AGC 114027	10	9.90	bTF	898	6.81	220	71
AGC 112454	9	10.2	mem	837	7.35	297	10
KDG 10	10	7.87	bs	953	7.66	297	126
UGC 1056	9	10.2	mem	774	8.54	375	-53
JKB 142	10	10.5	bTF	887	7.01	403	60
UGC 1104	9	7.55	bs	869	8.35	481	42
NGC 891	3	9.95	trgb	736	10.98	0	0
[TT2009] 25	10	10.28	trgb	903	7.23	43	167
[TT2009] 30	10	9.95	mem	—	6.79	62	—
NGC 1291	1	9.08	trgb	702	10.97	0	0
NGC 1291 Dw3	-1	9.08	mem	—	7.84	24	—
NGC 1291 Dw6	-1	9.08	mem	—	7.46	49	—
NGC 1291 Dw2	-1	9.08	mem	—	7.60	98	—
NGC 1291 Dw8	-1	9.08	mem	—	8.10	98	—
NGC 1291 Dw5	-1	9.08	mem	—	7.72	98	—
NGC 1291 Dw4	-1	9.08	mem	—	7.81	98	—
NGC 1291 Dw13	-1	9.08	mem	—	7.28	114	—
NGC 1291 Dw15	10	9.08	mem	—	6.30	133	—
NGC 1291 Dw12	-1	9.08	mem	—	6.52	184	—
NGC 1291 Dw1	-1	9.08	mem	—	7.38	185	—
[KK2000] 08	9	9.08	mem	—	7.64	195	—
ESO 300-014	8	9.80	TF	824	9.30	230	122
NGC 1291 Dw9	-1	9.08	mem	—	7.04	241	—
NGC 1291 Dw10	-1	9.08	mem	—	7.58	260	—
NGC 1291 Dw14	10	9.08	mem	—	6.60	274	—
ESO 300-4016	10	9.61	trgb	583	7.94	279	-119
NGC 1291 Dw11	10	9.08	mem	—	6.86	312	—
IC 342	6	3.28	cep	244	10.60	0	0
KK 35	10	3.16	trgb	149	7.97	15	-95
UGCA 86	8	2.98	trgb	280	9.13	89	36
KKH 22	-1	3.12	trgb	251	6.70	228	7
NGC 1560	7	2.99	trgb	170	8.60	312	-74
NGC 1569	8	3.19	trgb	106	9.40	312	-138
Cam A	10	3.56	trgb	156	7.79	326	-78
Cam B	10	3.50	trgb	267	7.09	365	23
UGCA 105	8	3.39	trgb	281	9.14	605	37
NGC 2683	3	9.82	trgb	365	10.81	0	0
NGC 2683 dw1	10	9.82	mem	334	6.49	34	-31
KK 69	10	9.16	trgb	418	7.27	65	53
NGC 2683 dw2	-2	9.82	mem	—	7.14	66	—

TABLE A1 Continued

TABLE A1 Continued

Name	T	D	meth	V_{LG}	$\log L_K$	R_p	ΔV
KK 70	-3	9.29	trgb	—	7.86	102	—
NGC 2784	-2	9.82	sbf	398	10.80	0	0
NGC 2784 dw1	-3	9.82	mem	—	8.41	7	—
KK 73	-1	9.82	mem	—	9.08	16	—
KSP-Dw18	9	9.82	mem	—	6.58	24	—
KK 72	-3	9.82	mem	—	7.83	35	—
KSP-Dw15	-2	9.82	mem	—	7.83	53	—
KSP-Dw14	-2	9.82	mem	—	7.84	80	—
KSP-Dw13	-2	9.82	mem	—	7.86	92	—
KSP-Dw20	-2	9.82	mem	—	7.45	94	—
KSP-Dw17	-1	9.82	mem	—	8.38	120	—
KSP-Dw12	10	9.82	mem	—	6.18	133	—
KK 74	-1	9.82	mem	—	8.52	137	—
KSP-Dw24	10	9.82	mem	—	6.58	171	—
KSP-Dw16	9	9.82	mem	—	6.66	176	—
KSP-Dw23	-2	9.82	mem	—	6.32	178	—
KSP-Dw21	-2	9.82	mem	—	6.45	180	—
KK 71	10	9.82	mem	—	7.46	183	—
DDO 56	10	10.91	TF	438	8.50	223	40
HIPASS J0916-23b	10	9.82	mem	550	8.47	223	152
KSP-Dw11	9	9.82	mem	—	7.16	224	—
KSP-Dw28	-1	9.82	mem	—	7.93	245	—
KSP-Dw30	10	9.82	mem	—	6.65	320	—
ESO 497-004	8	11.17	TF	519	8.85	367	121
NGC 2835	5	10.30	TF	600	10.19	382	202
KSP-Dw6	-2	9.82	mem	—	6.99	390	—
DDO 62	8	10.86	bTF	560	8.71	459	162
KSP-Dw3	-2	9.82	mem	—	8.22	560	—
KSP-Dw4	10	9.82	mem	—	7.72	566	—
KSP-Dw1	-1	9.82	mem	—	7.80	626	—
NGC 2903	4	9.17	trgb	443	10.85	0	0
UGC 5086	-3	8.70	sbf	378	8.34	23	-65
NGC 2903-HI	10	9.17	mem	470	6.94	65	27
KDG 56	10	9.17	mem	441	7.44	245	-2
LSBC D565-06	10	9.29	trgb	386	7.34	460	-57
AGC 198508	10	10.42	trgb	424	7.23	630	-19

TABLE A1 Continued

Name	T	D	meth	V_{LG}	$\log L_K$	R_p	ΔV
M81 = NGC 3031	3	3.70	trgb	104	10.95	0	0
Holm IX	10	3.85	trgb	192	7.75	12	88
BK3N	10	4.17	trgb	101	6.12	12	-3
JKB3	10	3.70	mem	198	5.63	17	94
A0952+69	10	3.93	trgb	242	6.87	18	138
Clump I	10	3.70	mem	-25	5.57	25	-129
KDG 61	-1	3.66	trgb	360	8.11	32	256
KDG 61em	10	3.70	mem	255	5.98	32	151
D0959+68	10	4.27	trgb	-46	6.44	35	-150
Clump III	10	3.70	mem	19	5.57	40	-85
M82	8	3.61	trgb	328	10.59	40	224
NGC 3077	9	3.85	trgb	159	9.57	49	55
Garland	10	3.82	trgb	183	6.81	53	79
FM1	-3	3.78	trgb	—	7.23	63	—
d0944+69	-3	3.84	trgb	—	5.88	64	—
BK5N	-3	3.70	trgb	—	7.18	73	—
d1006+69	-3	4.33	trgb	—	6.30	77	—
IKN	-3	3.75	trgb	-1	7.60	85	-105
d1005+68	-2	3.98	trgb	—	5.92	85	—
d1009+68	-3	3.73	trgb	—	6.25	85	—
d0955+70	-3	3.45	trgb	—	6.48	88	—
NGC 2976	7	3.66	trgb	142	9.44	89	38
KDG 64	-3	3.75	trgb	121	7.99	105	17
KK 77	-3	3.80	trgb	—	7.84	108	—
d1015+69	-1	4.07	trgb	—	6.06	114	—
d1014+68	-1	3.84	trgb	—	6.12	115	—
F8D1	-3	3.75	trgb	8	7.98	120	-96
d0934+70	-3	3.02	trgb	—	6.64	137	—
d1006+67	-3	3.61	trgb	—	6.31	140	—
d0958+66	9	3.82	trgb	221	7.12	145	117
HIJASS	11	3.70	mem	187	—	150	83
Holm I	10	4.02	trgb	291	8.05	159	187
d0944+71	-1	3.47	trgb	115	7.41	166	11
d0939+71	10	3.65	trgb	—	5.60	167	—
KDG 63	-3	3.65	trgb	0	7.84	172	-104
d0926+70	10	3.40	trgb	—	6.11	180	—
HS 117	10	3.96	trgb	116	6.72	195	12

TABLE A1 Continued

Name	T	D meth	V_{LG}	$\log L_K$	R_p	ΔV
IC 2574	8	3.93 trgb	183	9.33	197	79
d1028+70	10	3.84 trgb	35	7.01	200	-69
DDO 78	-3	3.48 trgb	191	7.48	205	87
DDO 82	9	3.93 trgb	207	8.39	219	103
d1041+70	-2	3.70 trgb	—	6.36	265	—
BK6N	-3	3.31 trgb	—	7.25	316	—
KDG 73	10	3.91 trgb	263	6.60	330	159
UGC 5497	9	3.73 trgb	267	7.19	340	163
KKH 57	-3	3.68 trgb	—	6.97	390	—
UGC 4483	10	3.58 trgb	304	7.09	520	167
DDO 53	10	3.68 trgb	150	7.34	525	46
Holm II	9	3.47 trgb	311	9.20	545	207
NGC 3115	-1	9.68 sbf	439	10.95	0	0
KDG 65	-3	9.70 mem	479	8.39	16	40
KKSG 18	-1	9.70 mem	456	9.27	48	17
KKSG 17	10	9.98 trgb	203	7.87	175	-236
MCG-01-26-009	10	9.70 mem	510	7.85	254	71
UGCA 193	7	9.70 mem	427	8.50	309	-12
KKSG 16	-3	9.70 mem	—	7.85	360	—
PGC 154449	9	9.70 mem	295	7.90	429	-144
LV J0956-0929	9	9.38 trgb	378	7.95	471	-61
KKSG 15	10	9.70 mem	554	8.24	487	115
NGC 3184	6	11.12 SN	588	10.52	0	0
LV J1018+4109	-1	11.12 mem	—	7.71	50	—
KUG1013+414	8	11.12 mem	513	8.32	90	-75
SDSS1028+42	10	10.28 NAM	551	7.33	445	-37
NGC 3521	4	10.70 TF	598	11.09	0	0
NGC 3521sat	-1	10.70 mem	—	8.62	30	—
KKSG 20	10	10.70 mem	636	7.37	56	38
NGC 3521 dw TBG	-2	10.70 mem	—	7.28	72	—
dw1110+0037	10	10.70 mem	669	7.25	252	71
KKSG 22	10	10.70 mem	—	7.11	265	—
UGC 6145	10	10.70 mem	546	7.83	341	-52
NGC 3556 = M108	6	9.90 TF	777	10.52	0	0

TABLE A1 Continued

Name	T	D meth	V_{LG}	$\log L_K$	R_p	ΔV
PGC 034671	9	9.90 mem	688	7.67	202	-89
NGC 4258 = M106	4	7.66 trgb	506	10.92	0	0
KDG 101	-1	7.28 trgb	330	8.41	29	-176
[KKH2011]s11	-3	7.66 mem	—	6.55	43	—
LV J1218+4655	8	8.28 trgb	477	7.49	53	-29
KK 132	-1	7.31 trgb	—	7.31	57	—
M106 edgeN4217	-2	7.70 mem	—	7.39	67	—
d1220+4649	-3	7.90 sbf	—	7.02	75	—
BTS 132	-3	7.40 sbf	—	7.36	119	—
NGC 4258 dwB	-2	7.66 mem	—	7.42	122	—
NGC 4288	7	8.24 NAM	588	8.63	141	82
DDO 120	9	7.28 trgb	516	8.73	206	10
NGC 4258 dwC	-2	7.66 mem	—	7.15	208	—
NGC 4242	7	7.62 trgb	568	9.47	228	62
NGC 4144	7	6.89 trgb	317	9.25	234	-189
UGC 7639	9	7.14 sbf	450	8.33	249	-56
LV J1203+4739	10	7.94 NAM	547	7.20	364	41
KK 133	10	8.32 NAM	601	7.04	525	95
KK 151	9	8.20 trgb	479	7.79	651	-27
NGC 4594 = M104	1	9.55 trgb	892	11.32	0	0
Suc D1	-1	9.55 mem	1109	7.39	7	217
dw1240-1140	-1	9.55 mem	1097	7.18	15	205
KKSG 32	-1	9.00 sbf	—	7.60	20	—
dw1239-1143	-1	7.90 sbf	1171	8.27	37	279
Sombrero-DwA	-1	9.70 sbf	—	6.99	47	—
Dw1241-1131	-1	7.20 sbf	—	6.98	47	—
dw1239-1152	-1	8.20 sbf	—	6.16	53	—
dw1240-1118	-1	8.80 sbf	—	8.53	53	—
Sombrero-DwB	-1	11.20 sbf	—	7.20	67	—
NGC 4594-DGSAT-3	-1	7.90 sbf	—	7.39	68	—
dw1239-1159	-1	11.3 sbf	—	7.32	70	—
KKSG 34	-1	9.00 sbf	—	7.80	73	—
dw1237-1125	-1	7.50 sbf	—	7.57	118	—
KKSG 33	-1	9.55 mem	—	7.59	122	—
PGC 042730	-1	9.55 mem	829	8.72	171	-63
KKSG 31	-1	9.55 mem	—	7.88	198	—

TABLE A1 Continued

Name	T	D meth	V_{LG}	$\log L_K$	R_p	ΔV
PGC 970397	10	10.0 TF	928	8.04	201	36
KKSG 29	10	9.82 trgb	562	7.67	220	-330
PGC 104868	9	11.17 TF	1171	8.23	362	279
NGC 4700	7	7.30 TF	1219	8.86	372	327
KKSG 30	10	9.72 trgb	918	7.71	471	26
UGCA 307	9	9.03 trgb	731	8.31	573	-161
NGC 4802	0	11.5 sbf	843	10.03	646	-49
PGC 044460	8	8.70 TF	1173	8.48	770	281
KKSG 27	9	6.64 bTF	1128	6.88	794	236
NGC 4818	2	11.3 TF	892	10.24	858	0
NGC 4597	8	10.10 TF	866	9.48	971	-26
NGC 4736 = M94	2	4.41 trgb	352	10.56	0	0
M94-Dw2	-1	4.70 trgb	—	6.59	40	—
M94-Dw1	-1	4.10 trgb	—	6.75	73	—
LV J1243+4127	10	4.81 trgb	444	6.77	105	92
KK 160	10	4.33 trgb	346	6.60	218	-6
IC 3687	10	4.57 trgb	377	8.19	238	25
IC 4182	8	4.35 trgb	357	8.70	350	5
NGC 4449	8	4.27 trgb	249	9.68	395	-103
KK 166	-3	4.39 trgb	—	7.21	429	—
CGCG 189-050	9	3.93 NAM	368	7.22	460	16
DDO 126	10	4.97 trgb	230	8.09	470	-122
DDO 168	10	4.25 trgb	270	8.13	496	-82
UGC 8215	10	4.57 trgb	304	7.18	501	-48
DDO 167	10	4.25 trgb	230	7.19	510	-122
NGC 4244	6	4.31 trgb	259	9.52	560	-93
DDO 169	10	4.41 trgb	348	7.73	600	-4
AGC 239141	10	3.75 NAM	359	6.01	602	7
NGC 4395	8	4.76 trgb	308	9.47	704	-44
MCG+06-27-017	9	4.85 trgb	341	7.89	717	-11
NGC 5055 = M63	4	9.04 trgb	570	11.00	0	0
TBGdw2	10	9.04 mem	—	6.51	57	—
KK 191	10	9.04 mem	—	6.83	63	—
UGC 8313	8	9.04 mem	658	8.46	65	88
KK 193	10	9.04 mem	—	6.71	85	—
TBGdw5	-1	9.04 mem	—	6.54	87	—

TABLE A1 Continued

Name	T	D meth	V_{LG}	$\log L_K$	R_p	ΔV
TBGdw3	-1	9.04 mem	—	6.26	88	—
KKH 82	10	7.48 NAM	545	7.46	92	-25
TBGdw6	10	9.04 mem	—	6.71	93	—
TBGdw7	-1	9.04 mem	—	6.22	95	—
TBGdw1	10	9.04 mem	—	6.51	102	—
TBGdw4	-1	9.04 mem	—	6.50	121	—
CGCG 217-018	9	9.04 mem	608	8.19	256	38
dw1308+40	-1	9.04 mem	—	7.54	278	—
dw1305+41	10	9.04 mem	—	7.28	306	—
dw1303+42	10	9.04 mem	—	6.88	374	—
KK 194	10	9.04 mem	—	7.15	387	—
SDSS132753	9	6.58 NAM	529	7.42	453	-41
NGC 5128 = Cen-A	-2	3.68 trgb	310	10.89	0	0
KV19-329	-1	3.68 mem	382	7.03	25	72
KV19-271	-1	3.68 mem	302	7.12	31	-8
CenA-MM-Dw7	-2	4.11 trgb	—	6.29	36	—
[KK2000] 55	-3	3.85 trgb	282	7.81	43	-28
KK 197	-3	3.84 trgb	388	8.12	51	78
KV19-212	-1	3.68 mem	286	7.02	61	-24
KV19-442	-1	3.68 mem	242	7.11	64	-68
CenA-MM-Dw3	-2	3.87 trgb	—	7.73	78	—
CenA-MM-Dw4	-2	4.09 trgb	—	6.95	84	—
CenA-MM-Dw9	-2	3.80 trgb	—	6.92	86	—
CenA-MM-Dw2	-2	4.15 trgb	—	6.17	91	—
CenA-MM-Dw1	-2	3.91 trgb	—	8.04	92	—
CenA-MM-Dw5	-2	3.61 trgb	—	5.59	93	—
ESO 324-024	8	3.78 trgb	272	8.35	102	-38
Fluffy	-1	3.68 mem	467	6.84	112	157
CenA-MM-Dw8	-2	3.47 trgb	—	6.49	122	—
dw1315-4309	-2	3.70 mem	—	5.74	127	—
CenA-MM-Dw6	-2	4.04 trgb	—	6.36	129	—
dw1315-4232	-2	3.70 mem	—	6.32	131	—
KK 196	10	3.96 trgb	490	7.14	138	180
dw1323-40b	-1	3.91 trgb	253	6.90	141	-57
dw1323-40	-1	3.73 trgb	207	7.01	143	-103
NGC 5237	9	3.33 trgb	122	8.43	143	-188
NGC 5011C	-1	3.73 trgb	394	7.98	145	84

TABLE A1 Continued

Name	T	D	meth	V_{LG}	$\log L_K$	R_p	ΔV
dw1329-45	-1	2.90	trgb	—	6.21	145	—
dw1337-41	-1	3.70	mem	—	6.49	145	—
dw1336-44	10	3.50	trgb	—	5.50	154	—
KK 189	-3	4.23	trgb	501	7.48	169	191
dw1331-40	-1	3.70	mem	—	5.79	186	—
ESO 269-066	-1	3.75	trgb	528	8.42	187	218
dw1341-43	-1	3.53	trgb	398	6.86	191	88
[KK2000] 57	-3	3.84	trgb	275	7.28	193	-35
dw1342-43	-1	2.90	trgb	273	6.61	204	-37
KK 203	10	3.77	trgb	57	6.50	207	-253
dw1322-39	10	2.95	trgb	413	6.12	207	103
KK 213	-3	3.77	trgb	—	7.52	217	—
KK 211	-2	3.68	trgb	360	7.75	237	50
ESO 325-011	10	3.40	trgb	311	7.86	244	1
KK 217	-3	3.50	trgb	—	7.22	295	—
ESO 269-058	9	3.75	trgb	140	8.86	307	-170
dw1330-38	-1	3.70	mem	—	6.16	313	—
[KK2000] 53	-3	2.92	trgb	—	7.46	317	—
dw1302-40	-1	3.70	mem	—	6.59	318	—
dw1257-41	-1	3.70	mem	—	7.13	330	—
ESO 269-037	10	3.15	trgb	481	6.96	333	171
NGC 5206	-3	3.21	trgb	334	8.95	345	24
dw1252-43	-1	3.70	mem	—	6.30	356	—
KK 221	10	3.82	trgb	268	6.74	368	-42
Cen-N	-3	3.66	trgb	—	7.32	389	—
NGC 5102	1	3.66	trgb	227	9.70	415	-83
[KK2000] 51	10	3.70	mem	—	6.60	439	—
dw1241-42	-1	3.70	mem	—	6.41	472	—
NGC 4945	6	3.47	trgb	299	10.66	474	-11
[KK2000] 58	-3	3.36	trgb	254	7.15	499	-56
dw1258-37	-1	3.70	mem	—	6.52	500	—
dw1240-42	-1	3.70	mem	—	6.86	500	—
ESO 383-087	8	3.19	trgb	108	9.05	539	-202
ESO 219-010	-3	4.29	sbf	—	8.03	562	—
ESO 174-001	10	3.60	TF	438	7.90	701	128
[KK2000] 54	10	3.75	trgb	394	6.26	723	84
PGC 051659	10	3.61	trgb	177	7.51	753	-133
NGC 5253	8	3.44	trgb	193	9.08	761	-117

TABLE A1 Continued

Name	T	D	meth	V_{LG}	$\log L_K$	R_p	ΔV
NGC 5194 = M51	5	8.40	SN	538	10.97	0	0
NGC 5195	0	7.66	sbf	548	10.59	12	10
NGC 5229	7	8.49	trgb	359	8.51	151	-179
dw1340+45	10	8.40	mem	—	6.74	342	—
LV J1328+4937	10	8.40	mem	497	7.20	349	-41
LV J1342+4840	9	8.40	mem	543	7.60	394	5
UGCA 361	-1	8.40	mem	—	8.13	409	—
MCG+08-25-028	10	8.40	mem	565	7.77	438	32
dw1313+46	10	8.40	mem	—	6.98	443	—
dw1338+50	-1	8.40	mem	—	7.08	485	—
dw1327+51	-1	8.40	mem	—	7.00	645	—
NGC 5236 = M83	5	4.90	trgb	307	10.86	0	0
KK 208	-3	5.01	trgb	—	8.71	27	—
UGCA 365	10	5.42	trgb	367	7.73	55	60
dw1340-30	-2	5.08	trgb	—	6.90	76	—
NGC 5264	8	4.79	trgb	269	8.88	86	-38
IC 4316	10	4.35	trgb	369	8.21	104	62
ESO 444-084	10	4.61	trgb	380	7.61	157	73
KK 218	-3	4.94	trgb	—	7.40	158	—
dw1328-29	-1	4.90	mem	—	6.75	159	—
dw1336-32	-2	4.90	mem	—	7.19	189	—
IC 4247	10	5.18	trgb	200	8.25	195	-107
dw1326-29	-2	4.90	mem	—	6.88	201	—
dw1330-32	10	4.90	mem	—	6.04	222	—
dw1329-32	9	4.90	mem	—	6.73	244	—
KK 200	10	4.76	trgb	271	7.31	249	-36
Dw1337-26	-2	4.90	mem	—	7.08	268	—
HIDEEP J1337-33	10	4.55	trgb	371	6.73	301	64
dw1337-33	10	4.90	mem	—	6.52	302	—
dw1325-33	-1	4.90	mem	—	6.78	305	—
KK 195	10	5.22	trgb	345	6.96	326	38
dw1321-27	-1	4.90	mem	—	6.79	335	—
dw1322-27	-1	4.90	mem	—	7.17	335	—
dw1341-33	-2	4.90	mem	—	7.06	342	—
dw1357-28	-1	4.90	mem	—	6.50	357	—
KK 198	-3	4.90	mem	—	7.39	393	—

TABLE A1 Continued

Name	T	D	meth	V_{LG}	$\log L_K$	R_p	ΔV
dw1314–28	–1	4.90	mem	—	7.25	439	—
dw1343–34	–1	4.90	mem	—	6.31	455	—
dw1401–32	–1	4.90	mem	—	6.87	458	—
dw1326–35	10	4.90	mem	—	6.14	479	—
dw1406–29	–1	4.90	mem	—	6.87	512	—
dw1403–33	–1	4.90	mem	—	6.75	525	—
dw1306–29	–1	4.90	mem	—	6.87	528	—
ESO 384–016	9	4.49	trgb	350	7.83	596	43
dw1301–30	–1	4.90	mem	—	6.72	601	—
dw1409–33	–1	4.90	mem	—	6.88	613	—
AM1320–230	–3	4.90	mem	—	7.46	619	—
dw1415–32	10	4.90	mem	—	6.08	680	—
dw1413–34	–1	4.90	mem	—	6.26	695	—
dw1410–34	10	4.90	mem	—	6.54	701	—
dw1318–21	–1	4.90	mem	—	7.06	781	—
HIPASS J1337–39	10	5.08	trgb	258	7.21	870	–49
M101 = NGC 5457	6	6.95	trgb	378	10.79	0	0
NGC 5477	9	6.77	trgb	451	8.26	44	73
M101-df1	10	6.37	trgb	—	6.17	53	—
NGC 5474	8	6.82	trgb	424	9.20	96	46
M101-df2	–1	6.87	trgb	—	6.74	96	—
M101-df3	–1	6.52	trgb	—	7.27	97	—
M101-DwA	–1	6.64	trgb	—	6.97	102	—
UGC 8882	–1	7.80	sbf	482	7.64	110	104
GBT1355+54	11	6.95	mem	345	—	152	–33
Holm IV	8	6.93	trgb	272	8.60	163	–106
M101-Dw9	–1	7.71	trgb	—	6.17	166	—
NGC 5585	7	7.00	trgb	457	9.07	429	79
dw1343+58	9	6.30	TF	338	7.65	605	–40
DDO 194	8	6.30	trgb	381	8.13	647	3
NGC 6744	4	9.51	trgb	706	10.91	0	0
[KK2000] 71	10	9.50	mem	—	8.24	30	—
[KK2000] 72	10	9.50	mem	—	7.12	50	—
[KK2000] 70	10	9.50	mem	—	7.21	55	—
NGC 6744 dw TBGb	10	9.50	mem	—	5.88	64	—
ESO 104–044	10	9.73	trgb	614	8.31	66	–92

TABLE A1 Continued

Name	T	D	meth	V_{LG}	$\log L_K$	R_p	ΔV
NGC 6744 dw TBGa	–1	9.50	mem	—	7.38	120	—
ESO 104–022	10	8.95	trgb	654	8.05	302	–52
AM1909–615	8	9.50	mem	821	7.92	333	115
NGC 6684	0	8.70	TF	720	10.39	435	14
IC 4870	9	8.51	trgb	740	8.34	592	34
NGC 6946	6	7.73	trgb	355	10.99	0	0
KK 251	10	7.73	mem	433	7.94	77	78
UGC 11583	10	7.30	trgb	429	8.16	86	74
KK 252	10	7.73	mem	441	8.13	105	86
KKR 55	10	7.73	mem	337	8.40	178	–18
KKR 56	10	7.73	mem	264	8.24	311	–91
Cepheus 1	8	7.73	mem	342	9.61	525	–13
KKR 59	8	7.73	mem	307	9.39	631	–48
KKR 60	10	7.73	mem	296	8.66	672	–59

These data are also available online at the CDS via <http://cdsarc.u-strasbg.fr/viz-bin/cat/J/AN/...>